

## Wavelet-like decomposition stage with windowed filters defined for the Discrete Trigonometric Transforms (DTTs)

**Abstract.** In the paper assumptions for a computational experiment along with obtained results leading to positive verification of the hypothesis about efficient Mallat scheme decomposition stage realization with use of the filters derived from the 16 DTTs, instead of the wavelet convolution filters, have been described. Introduction of windowing in the time domain resulted in considerable reduction of computations, up to 34 times, while the accompanying distortion has been assessed at the PSNR level about 40dB. The investigation was performed with statistically defined signals, based on the first-order Markov process with assumed intersymbol correlation.

**Streszczenie.** W artykule opisano założenia oraz wyniki eksperymentu obliczeniowego pozytywnie weryfikującego hipotezę o możliwości efektywnego zrealizowania etapu dekompozycji według schematu Mallata przy zastąpieniu spłotowych filtrów zafalowaniowych filtrami pochodzącymi z 16 dyskretnych transformacji trygonometrycznych. Zastosowanie okien w dziedzinie czasu pozwoliło na zmniejszenie ilości obliczeń do 34 razy, przy wprowadzeniu nieznacznych deformacji sygnału, oszacowanych na poziomie około 40dB (PSNR). Badania przeprowadzono dla sygnałów zdefiniowanych statystycznie z wykorzystaniem procesów Markowa pierwszego rzędu z założoną wartością korelacji międzysymbolowej. (Dekompozycja w schemacie zafalowaniowo-podobnym z wykorzystaniem okienkowanych filtrów określonych dla dyskretnych transformacji trygonometrycznych).

**Keywords:** Discrete Wavelet Transform, Discrete Cosine Transform, Discrete Sine Transform, generalized convolution.

**Słowa kluczowe:** dyskretna transformacja zafalowaniowa, dyskretna transformacja kosinusowa, dyskretna transformacja sinusowa, spłot uogólniony.

### Introduction

Transforms with sine and cosine kernels belong to the important area of signal analysis, they are used mainly in the compression field, spectral analysis and transform domain processing of real signals [1,2,3]. All of such transforms with discrete domain are named the Discrete Trigonometric Transforms (DTT). While there is only one continuous sine and one cosine transform, in the discrete domain there exists some variety of orthonormal solutions. In general, the DTT of a signal sequence  $x$  may be described as

$$(1) \quad \hat{x}(k) = a_k \sum_{n=0}^{N-1} b_n x(n) \text{kernel}(n, k) \quad \text{for } k = 0, \dots, N-1$$

where *kernel* may be either sine or cosine function. The different versions of DTTs are obtained with adding 0.5 to the selected indexes, and relevant adjusting  $a$  and  $b$  coefficients to preserve orthonormality. There are four even Discrete Cosine Transforms (DCTs), four odd DCTs, four even Discrete Sine Transforms (DSTs), and four odd DSTs. Within each group they are named as type: I, II, III and IV. For example the orthonormal Discrete Cosine Transform (DCT) of type I even (DCT Ie) is defined as

$$(2) \quad \hat{x}(k) = c_k \sqrt{\frac{4}{2(N-1)}} \sum_{n=0}^{N-1} c_n x(n) \cos(2\pi nk / (2(N-1)))$$

$$\text{for } k = 0, \dots, N-1$$

$$c_m = \begin{cases} 1/\sqrt{2} & \text{for } m = 0 \text{ or } m = N-1, \\ 1 & \text{otherwise} \end{cases}$$

while the DCT of type III even (DCT IIIe) is

$$(3) \quad \hat{x}(k) = \sqrt{\frac{4}{2N}} \sum_{n=0}^{N-1} c_n x(n) \cos(2\pi n(k+0.5)/(2N))$$

$$\text{for } k = 0, \dots, N-1$$

$$c_m = \begin{cases} 1/\sqrt{2} & \text{for } m = 0, \\ 1 & \text{otherwise} \end{cases}$$

Interesting practical property of the DTT family is that its members are mutually related when we consider the inverse transform. For example, for the DCT II even the inverse is the DCT III even, and for the DCT I even the same transform is its inverse. Further detailed description may be found in [3,4].

From now on, to simplify the reference, the 16 DTTs will be numbered as indicated in Table 1

Table 1.  $M$  numbers of DDTs

DTT	$M$	DTT	$M$
DCT Ie	1	DST Ie	9
DCT IIe	2	DST IIe	10
DCT IIIe	3	DST IIIe	11
DCT IVe	4	DST IVe	12
DCT Io	5	DST Io	13
DCT Ilo	6	DST Ilo	14
DCT IIIo	7	DST IIIo	15
DCT IVo	8	DST IVo	16

In [5,6], it was shown, that the well known wavelet-based decomposition scheme proposed by Mallat [7], and applied in subband coding [8,9,10,11,12], originally designed for FIR filters, related to their characteristics in the Fourier domain, may be efficiently used for the DTT-based filters. For four, out of the sixteen DTTs, the reconstruction proved to be perfect, and for the remaining transforms some generalized approach, exploiting matrix representation, helped to solve the task. In this paper the further, recently obtained results are presented, describing an experiment designed to study the reconstructed signal quality after applying windows directly in the time domain, and thus enabling considerable reduction of the number of computations in the decomposition stage.

### The decomposition scheme

Figure 1 a) shows the considered system, directly derived from the well-known Mallat scheme. Blocks with  $f_L$  and  $f_H$  represent the decomposition filters, while  $g_L$  and  $g_H$  the synthesis filters, with relevantly applied down- and up-sampling. However, in the considered case the filtering is

not performed with the Fourier-based FIR filters [8,13], but with the DTT-based pseudo-convolutional filters, proposed in [14] and developed gradually in [4,15,16,17,18]. We concentrate on the decomposition stage, as the synthesis stage is assumed to be ideal thus guaranteeing the perfect reconstruction. Such feature has been obtained with the matrix representation representing the relevant operations – cf. Figure 1 b) and c), and formula (1).

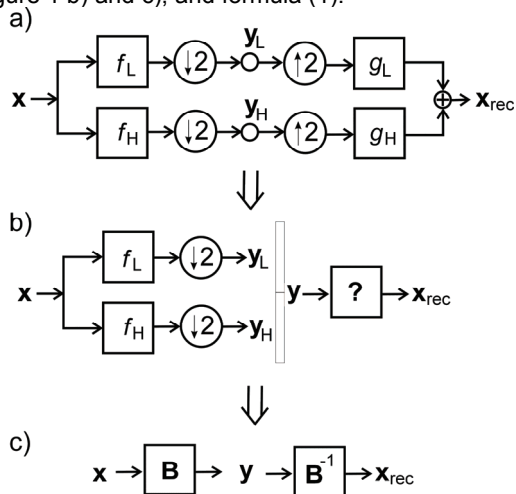


Fig. 1. Schematic diagram of one level of the wavelet-like decomposition used in this paper (cf. [9,10]): a) basic diagram, b) hypothesis about the perfect reconstruction formulated using matrix notation, c) solution – cf. (1)

Let  $\mathbf{x}$  and  $\mathbf{y}$  be vectors (signal blocks) of size  $N \times 1$ . Then

$$(4) \quad \mathbf{y} = \mathbf{B}\mathbf{x}, \quad \text{where} \quad \mathbf{B} = \begin{bmatrix} \mathbf{D}_N \mathbf{Q}_L \\ \mathbf{D}_N \mathbf{Q}_H \end{bmatrix},$$

in which  $\mathbf{D}_N$  is the downsampling matrix of size  $(N/2) \times N$  and  $\mathbf{Q}_L$   $\mathbf{Q}_H$  are the generalized convolution matrices of size  $N \times N$  for the ideal lowpass and the highpass filter, respectively. The ideal half-band filter is defined in the transform domain, and consists only from 1s and 0s, while 1s cover the relevant passband. The convolution matrices have been obtained from the transform matrix  $\mathbf{A}$  and the relevant diagonal matrices  $\mathbf{H}_L$  and  $\mathbf{H}_H$  containing on their diagonals respective filter coefficients defined in the transform domain [6], i.e.

$$(5) \quad \begin{aligned} \mathbf{Q}_L &= \mathbf{A}^{-1} \mathbf{H}_L \mathbf{A} \\ \mathbf{Q}_H &= \mathbf{A}^{-1} \mathbf{H}_H \mathbf{A} \end{aligned}$$

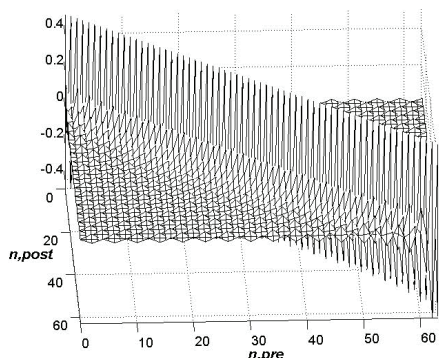


Fig. 2. A 3-D mesh graph of the  $\mathbf{Q}_L$  matrix for the DCT 1e ( $M = 1$ ) confirming that such matrix is suitable for windowing along its rows, with the window sliding accordingly along variable  $n$

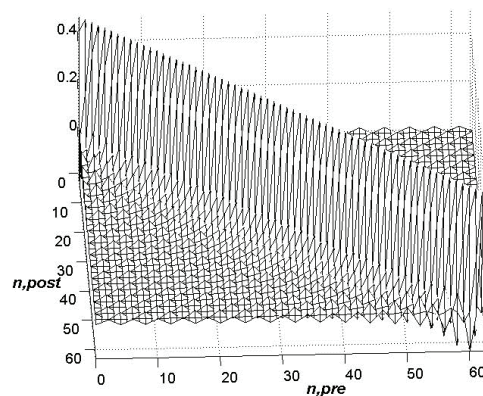


Fig. 3. A 3-D mesh graph of the  $\mathbf{Q}_H$  matrix for the DCT 1e ( $M = 1$ ) confirming that such matrix is suitable for windowing along its rows, with the window sliding accordingly along variable  $n$

As an example, Figures 2 and 3 present in the 3-D mesh form  $\mathbf{Q}$  matrices, obtained for the half-band filters and the DCT 1e ( $M = 1$ ), for the signal block length  $N = 64$ , indicating that the largest coefficients are localized around the diagonal. For the remaining DDTs the  $\mathbf{Q}$  matrices have the same property [17,18].

### Windowing

Because for all DTTs the largest values of  $\mathbf{Q}$  matrices are located around the diagonals, the windowing, as described in [17,18], should efficiently reduce the required number of computations without introducing large error. Four type of windows were selected for this study: 1) rectangular (see Figure 4), 2) triangular, 3) Hann, and 4) Hamming (see Figure 5).

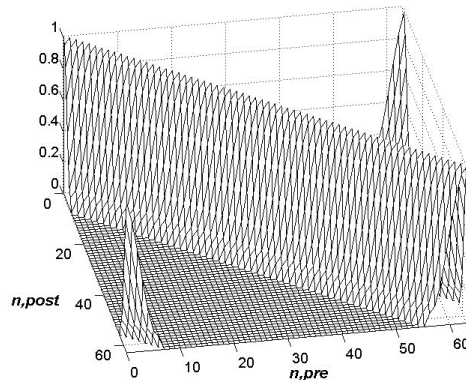


Fig. 4. Window matrix  $\mathbf{W}_1$  designed for rectangular window of length  $W = 15$ , while signal block is  $N = 64$

Figures 4 and 5 present examples of the windowing  $\mathbf{W}$  matrices used to multiply  $\mathbf{Q}$  matrices term-by-term to obtain the windowed filters (a windowed filter can be obtained by multiplication of the original  $\mathbf{Q}$  matrix by the window matrix  $\mathbf{W}$ , i.e.

$$(6) \quad \mathbf{Q}^w = \mathbf{Q} \otimes \mathbf{W},$$

where  $\otimes$  denotes the term-by-term multiplication).

The discussed windows were applied to both, low- and highpass, half-band filters. Because the results for both types of filters were practically the same, only those for the lowpass filters are presented below.

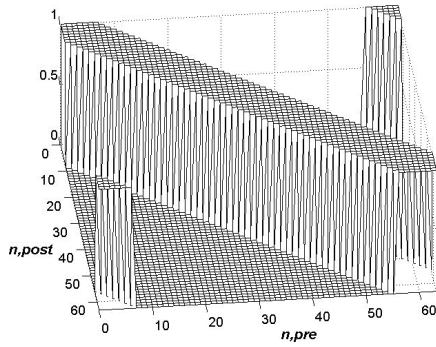


Fig. 5. Window matrix  $W_4$  designed for the Hamming window of length  $W = 15$ , while signal block is  $N = 64$

To evaluate and compare the results an error measuring technique has been adopted from [3]. Accordingly, the signal was assumed to be realization of the Markov-1 process with zero mean, unit variance, and assumed correlation coefficient,  $\rho$ , between consecutive elements – see Figure 6 for examples of such realizations.

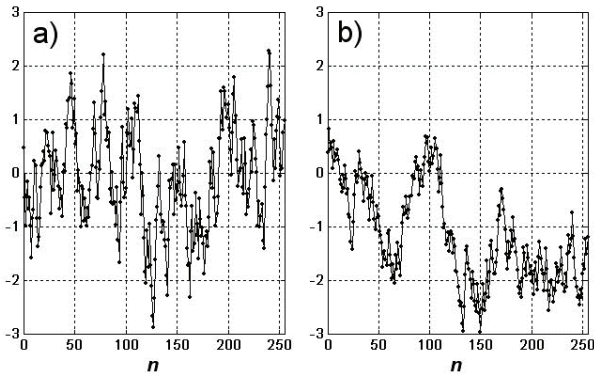


Fig. 6. Examples of realization of the Markov-1 process with zero mean, unit variance, and: a)  $\rho = 0.80$ , b)  $\rho = 0.95$ ; signal block length:  $N = 256$

Then the error was computed in a form of the MSE (mean square error) in relation to the non-windowed filters taken as reference. In this process the assumed intersymbol correlation leads to the following covariance matrix [3]

$$(7) \quad \mathbf{R}_\rho : R(i, j) = \rho^{|i-j|}$$

Then, two matrix operators,  $\mathbf{X}$  and  $\mathbf{Y}$ , both alternatively used to multiply the signal block of length  $N$ , may be compared with the following formula for the MSE statistically comparing the resulting signal blocks [3]

$$(8) \quad \text{MSE} = \frac{1}{N} \text{trace}((\mathbf{X} - \mathbf{Y})\mathbf{R}_\rho(\mathbf{X} - \mathbf{Y})^T)$$

In Figures 7 and 8 the resulting MSE values for the following  $\rho = 0.5, 0.6, 0.7, 0.8, 0.95$ , and two types of windows, are presented. For the remaining windows the trends were the same, while the MSE values were larger than for the Hamming window.

Note, that the obtained MSE values are relatively small, however, the rectangular window provides better performance than the remaining windows. Additionally, there is a noticeable, linear, sensitivity to  $\rho$ , and there is also very little difference between particular DTTs. For more intuitive judgment it may help if we recall that the peak-to-peak distance for the Gaussian distribution with variance equal to 1 is typically assumed to be 6. Then, the PSNR

(peak signal to noise ratio) for  $\text{MSE} = 0.001$  is 45.6 dB, which is typically considered imperceptible in the area of image lossy compression [19]. Similarly,  $\text{MSE} = 0.01$  is equivalent to 35.6 dB, which is still a quite good result.

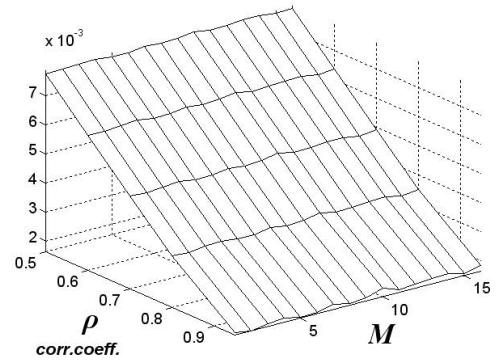


Fig. 7. Statistical MSE values obtained for the rectangular window (numbered as 1) of length  $W = 15$ ,  $N = 256$

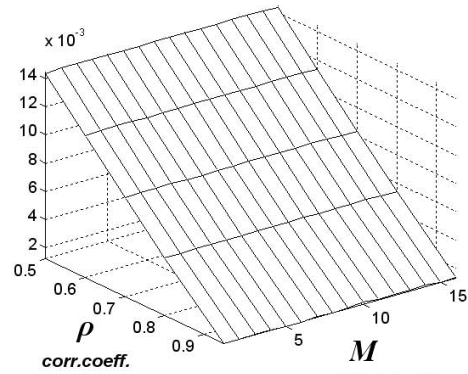


Fig. 8. Statistical MSE values obtained for the Hamming window (numbered as 4) of length  $W = 15$ ,  $N = 256$

Afterwards, the same methodology was utilized for the whole decomposition stage, including both filters, each windowed separately, and then downsampled (1). Figures 9 and 10 present the resulting MSE for  $\rho = 0.8$  and  $\rho = 0.95$ , respectively. The results indicate that the mutual relationship depends heavily on the assumed value of  $\rho$  in the Markov model, however, in all cases the best results were obtained for either the rectangular or Hamming window.

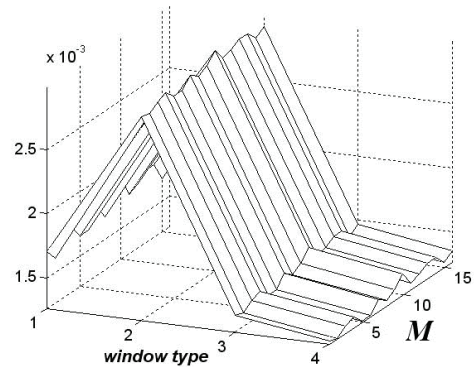


Fig. 9. Statistical MSE values for all four window types and DTTs, for the signal resulting from the Markov-1 model with  $\rho = 0.8$ ,  $W = 15$ ,  $N = 256$

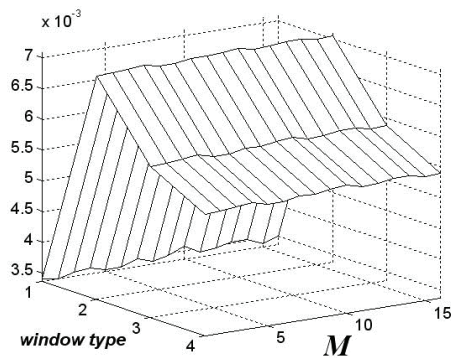


Fig. 10. Statistical MSE values for all four window types and DTTs, for the signal resulting from the Markov-1 model with  $\rho = 0.95$ ,  $W = 15$ ,  $N = 256$

### The multivariable comparison

The presented study, with several varying variables, indicated that the mutual relationship may be more sophisticated than it may seem from the sole graph. Therefore, the comparative computations were arranged with five varying parameters: 1) Markov process correlation coefficient,  $\rho = 0.8$  and  $\rho = 0.95$ ; 2) window length,  $W = 15, 31, 63$ ; 3) signal block length,  $N = 64, 128, 256, 512$ , 4) window type, rectangular or Hamming, and 5) DTT type (sixteen transforms). The results are presented in Figure 11.

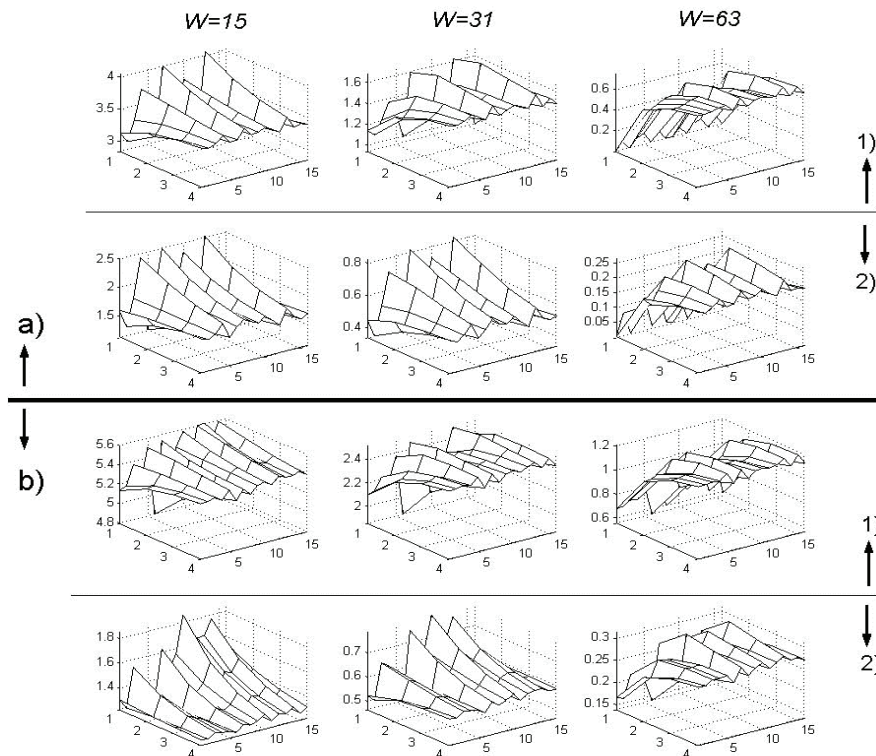


Fig. 11. Comparison of the statistical MSE values, here multiplied by 1000, for different length values of a window:  $W = 15, 31, 63$ , and signal blocks:  $N = 64, 128, 256, 512$  (indicated respectively by numbers on one horizontal axis from 1 through 4) and all DTTs (numbered on the other horizontal axis from 1 to 16), obtained for the assumed Markov process, with: a) rectangular window, b) Hamming window, and for: 1)  $\rho = 0.80$ ; 2)  $\rho = 0.95$ . The arrows indicate groups of graphs related to given set of options, for example, the first row of three graphs corresponds to a) and 1)

The study indicates that for long  $N$  all the DTTs become similar, in spite of the fact that they behave differently for short blocks, and the MSE values approach some saturation value. The Hamming window does not improve the performance as compared to the rectangular window, and for  $\rho = 0.8$  it makes the results considerably worse. Note, however, that all results indicate PSNR above 35 dB, while for signal model based on  $\rho = 0.95$  and window with length  $W = 63$  ( $N = 512$ ) the PSNR exceeds 51 dB.

### The wavelet-like interpretation and impact of windowing

While investigating the wavelet-like decomposition it was tempting to verify the shape of the basis functions, being equivalent to scaling and wavelet function in the classical wavelet analysis. Five-level decomposition was assumed and all transform coefficients were set to zero except one within the last level, which was set to '1'. Then the reconstruction was performed. When '1' was placed in the lowpass half, it resulted in the scaling-like function, and

when it was in the highpass part, then we obtained the wavelet-like function.

As the results were very similar for all DTTs, we selected the DCT 1e to provide examples. To emphasize the differences between classical Fourier-based analysis, and the discussed option, the '1' was located in two different locations: at the beginning of the relevant block and close to its centre. The resulting comparison clearly indicates that the function shape depends on the location of '1', which is the immediate result of the fact that the DTTs do not have the shifting property. Moreover, the relevant transform of the functions (here, the DCT 1e), indicates the change in the filters shape in the transform domain, however, keeping the division into the lowpass and bandpass, as expected for the classical Fourier-based wavelet decomposition.

Figures 12 and 13 depict the functions and their transforms, which could be compared with the well known wavelet features [9,11,12]. In this study the complete decomposition filters were assumed, however, consecutive Figures 14, 15, 16, and 17 present results after allowing the

use of windows: first rectangular, then Hamming, and the visual results indicate, that the relevant windowing, instead of the simplest rectangular, may be still of some importance and bring some benefit. But obviously, the relevantly profound study should be performed separately and is beyond the scope of this paper.

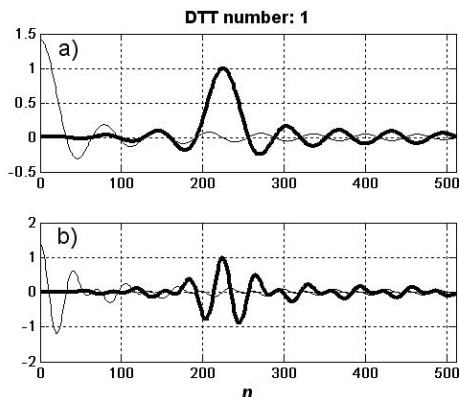


Fig. 12. Examples of functions equivalent to: a) scaling-like function, b) wavelet-like function, obtained for DCT Ie, and five-level reconstruction scheme. Thick line depicts the functions obtained for '1' in the middle of the transform, and thin line for '1' located at the initial sample (no windowing was used)

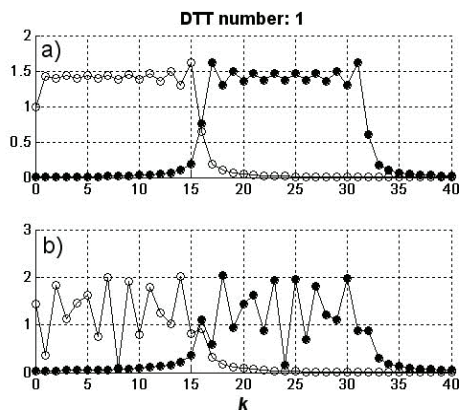


Fig. 13. Transforms computed with DCT Ie for the functions from Figure 12: a) scaling-like (○) and wavelet-like (●) for '1' at the beginning, b) scaling-like (○) and wavelet-like (●) for '1' in the middle

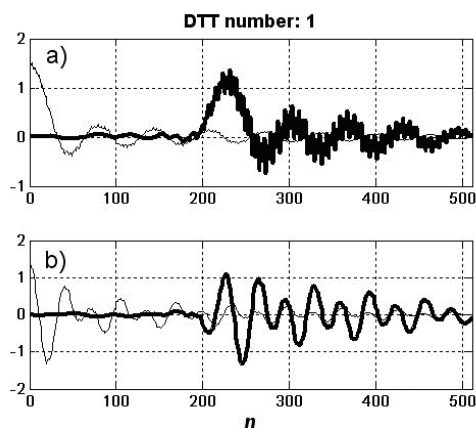


Fig. 14. Graphs obtained and presented in the same manner as in Figure 12, but using rectangular window with  $W = 15$  in the decomposition stage

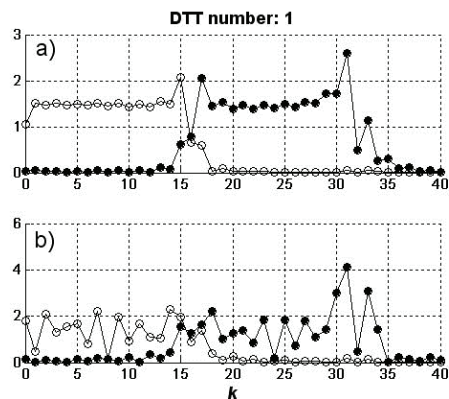


Fig. 15. Transforms computed with DCT Ie for the functions from Figure 14, depicted as in Figure 13

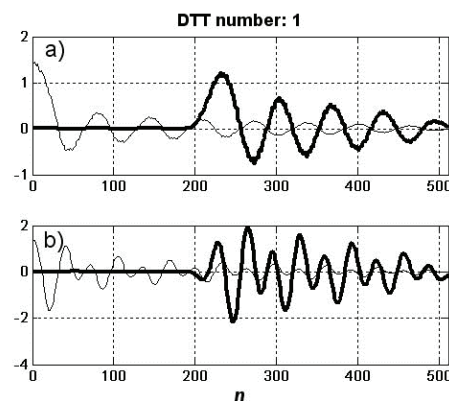


Fig. 16. Graphs obtained and presented in the same manner as in Figure 12, but using the Hamming window with  $W = 15$  in the decomposition stage

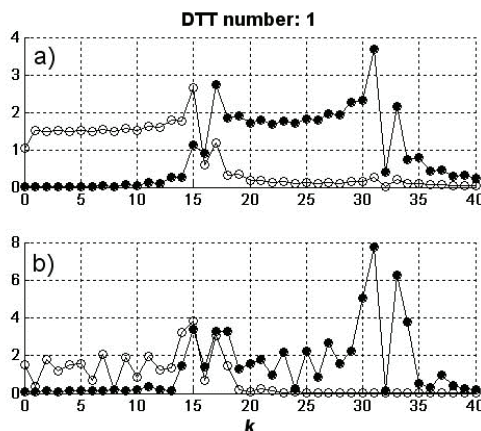


Fig. 17. Transforms computed with DCT Ie for the functions from Figure 16, depicted as in Figure 13

### Concluding comments

The described study indicates that the rectangular window used to reduce the filter matrix applied in time domain enables considerable reduction of computations – up to 34 times (for  $N = 512$  and  $W = 15$ ), when compared to complete matrix operation (4).

Introducing the DTT-based wavelet-like transform values, the error measured statistically with the PSNR was obtained within the range from 36 dB up to even more than 51 dB. The proposed scheme preserves also the subband decomposition property, as for the Fourier-based technique.

The study shows that the DTT-based decomposition scheme mimicking the classical wavelet Fourier-based procedure exhibits features in many aspects similar to those of the classical technique. Therefore, investigation of this

concept should be continued to define practical conditions for efficient applications. However, the results that have been obtained so far, both presented in [9,10] and in this study, should already encourage the use of DTTs as a tool in similar areas, in which common Fourier-based wavelet decomposition scheme is typically applied, like feature extraction, noise reduction or compressive coding.

*On the part of Przemysław Korohoda this work was supported by the AGH University of Science and Technology grant no. 11.11.120.766.*

#### REFERENCES

- [1] Ahmed N., Rao K.R., Orthogonal Transforms for Digital Signal Processing, *Springer-Verlag* (1975)
- [2] Yip P., Sine and Cosine Transforms, in *The Transforms and Applications Handbook*, 2<sup>nd</sup> Ed., edited by Poularikas A.D., CRC Press, IEEE Press (2000), 3,1-66
- [3] Britanak V., Yip P., Rao K.R., Discrete Cosine and Sine Transforms – General Properties, Fast Algorithms and Integer Approximations, *Elsevier, Academic Press* (2007)
- [4] Korohoda P., Dąbrowski A., Generalized convolution as a tool for the multi-dimensional filtering task, *Multidimensional Systems and Signal Processing*, 19 (2008), 361-377
- [5] Korohoda P., Dąbrowski A., Experimental study of wavelet-like decomposition based on filtering in domains of discrete trigonometric transforms, *Proceedings of the IEEE workshop on Signal Processing: Algorithms, Architectures, Arrangements, and Applications (SPA 2010)*, Poznań, Poland (2010), 16-20
- [6] Korohoda P., Dąbrowski A., Wavelet-like decomposition based on filtering in domains of discrete trigonometric transforms – case study, *Elektronika*, 52 (2011), 5, 85-89
- [7] Mallat S.G., A theory for multiresolution signal decomposition: The wavelet representation, *IEEE Transactions on Pattern Analysis and Machine Intelligence*, 11 (1989), 674-693
- [8] Proakis J.G., Manolakis D.G., Digital Signal Processing: Principles, Algorithms, and Applications, *Prentice Hall*, 3rd Ed. (1996)
- [9] Strang G., Nguyen T., Wavelets and Filter Banks, *Wellesley College*, 2<sup>nd</sup> Ed. (1996)
- [10] Vaidyanathan P.P., Multirate Systems and Filter Banks, *Prentice Hall* (1992)
- [11] Vetterli M., Herley C., Wavelets and Filter Banks: Theory and Design, *IEEE Transactions on Signal Processing*, 40 (1992), 9, 2207-2231
- [12] Vetterli M., Kovačević J., *Wavelets and Subband Coding*, Prentice Hall (1995)
- [13] Mitra S.K., Digital Signal Processing: A Computer Based Approach, *McGraw-Hill* (1998)
- [14] Korohoda P., Dąbrowski A., Generalized primary domain interpretation of product filtering of digital signals in the transform domain, *Proceedings of Signal Processing*, (Poznań, Poland), (2003), 75-80
- [15] Korohoda P., Dąbrowski A., Fast filtering by generalized convolution related to discrete trigonometric transforms, *Proceedings of the IEEE workshop on Signal Processing: Algorithms, Architectures, Arrangements, and Applications (SPA 2007)*, Poznań, Poland (2007), 57-62
- [16] Korohoda P., Dąbrowski A., Digital filtering by discrete trigonometric transforms realized with generalized convolution, *Elektronika*, 48 (2008), 4, 95-98
- [17] Korohoda P., Dąbrowski A., Lowpass filtering with filters defined in the discrete trigonometric transform domains, *Proceedings of the IEEE workshop on Signal Processing: Algorithms, Architectures, Arrangements, and Applications (SPA 2009)*, Poznań, Poland (2009), 66-69
- [18] Korohoda P., Dąbrowski A., Discrete trigonometric transforms (DTT) filters, *Elektronika*, 51 (2010), 3, 45-49
- [19] Rao K.R., Kim D.N., Hwang J.J., Fast Fourier Transform: Algorithms And Applications, *Springer-Verlag* (2010)

**Authors:** dr inż. Przemysław Korohoda, AGH University of Science and Technology, Department of Electronics, Faculty of Electrical Engineering, Automatics, Computer Science and Electronics, al. Mickiewicza 30, 30059 Kraków, E-mail: [korohoda@agh.edu.pl](mailto:korohoda@agh.edu.pl) ; prof. dr hab. inż. Adam Dąbrowski, Poznań University of Technology, Department of Control and System Engineering, Faculty of Signal Processing and Electronic Systems, ul. Piotrowo 3a, 60-965, E-mail: [Adam.Dabrowski@put.poznan.pl](mailto:Adam.Dabrowski@put.poznan.pl) .